Hindawi
Advances in Materials Science and Engineering
Volume 2022, Article ID 6804011, 13 pages
https://doi.org/10.1155/2022/6804011

Research Article

Effect of TaC/Ti/Si_3N_4 Hard Ceramics on Mechanical and Microstructural Behaviour of AA7075 Processed through Stir Casting Process

J. Pradeep Kumar,[1] **D. S. Robinson Smart**,[2] **Stephen Manova**,[1] **and N. Ummal Salmaan**[3]

[1]*Department of Mechanical Engineering, Karunya Institute of Technology and Sciences, Coimbatore 641114, Tamilnadu, India*
[2]*Department of Aerospace Engineering, Karunya Institute of Technology and Sciences, Coimbatore 641114, Tamilnadu, India*
[3]*Department of Automotive Engineering, Aksum University, Axum, Ethiopia*

Correspondence should be addressed to N. Ummal Salmaan; ummalsalmaan90@gmail.com

Received 10 February 2022; Revised 5 March 2022; Accepted 4 April 2022; Published 21 April 2022

Academic Editor: Adam Khan M

A liquid metallurgical stir casting route was utilized for developing aluminium alloy (7075) matrix composites blended with fluctuating wt% of silicon nitride (Si_3N_4), tantalum carbide (TaC), and titanium (Ti) for sake of generating a profitable composite with enhanced properties. The physical, microstructural, and mechanical characteristics such as density, high temperature tensile, fatigue, and time-dependent creep experiments were conducted and evaluated. SEM microstructural examinations were performed on the composite samples and proved that there was a good interfacial bonding and uniform dissemination among the reinforcement particulates in the matrix. Physical characteristics were analysed and the outcomes showed that AA7075 blended with 1 wt% TaC, 8 wt% Si_3N_4, and 0.5 wt% Ti proved higher experimental and theoretical densities of 3.2464 g/cm^3 and 3.3038 g/cm^3, respectively, with maximum porosity of 1.7758%. At 30°C, the tensile properties of the developed MMCs showed improved ultimate tensile strength (UTS) of 137.64 N/mm^2. Beyond 100°C, AA7075 reinforced with 0.75 wt% TaC, 6 wt% Si_3N_4, and 1 wt% Ti proved to have a higher strength of 232.17 N/mm^2. Fatigue properties of the developed MMCs discovered were found to be reformed when proportionate to the base alloy by operating at 14×10^3 cycles at the stress of 42.72 MPa. Time-dependent creep analysis of the developed MMCs found to be advanced due to the addition of tough ceramic particulates.

1. Introduction

Human capabilities are the key to realizing the potential of materials. Progression of materials is only possible through the continuous improvement of human behaviour and science [1]. The betterment of novel lightweight structural composites with exceptional mechanical behaviour is a productive methodology to improve the energy effectiveness of components used in military, defence, aerospace, armor, and automotive applications for enhancing reducing CO_2 emissions and fuel efficiency through a reduction in weight of interior and exterior components. These hard ceramic materials gain importance in turbine and aircraft industries and their components such as turbine blades, rivets, and aircraft outer components that are exposed to elevated atmospheric conditions [2]. Lightweight aluminium metal matrix composites (MMCs) are of immense attention in the present situation as a consequence of their high-level electrical, thermal, and mechanical aspects [3]. Properties such as exceptional toughness, higher stiffness and strength, low specific gravity and coefficient of thermal expansion, good wear and corrosion inheritance, high thermal conductivity, and high dimensional accuracy shifted the research from monolithic material to the composites [4]. The MMCs are amalgamations of two or more distinct materials with one being metal and the other being hard ceramics. When not less than two or more than two reinforcements are assimilated, then it is designated as hybrid composites [5]. MMCs are extensively used in various product development such as camera domes, wheel covers, rivets, turbine blades,

and so on in critical applications such as automobile, turbine sectors, aerospace, defence, and military [6]. Recently, there has been a spreading curiosity about using MMCs for high-temperature applications, especially under creep conditions, in aircraft and automobile engines technologies [7]. Particulate blended MMCs have numerous benefits, and it was manufactured certainly with minimal cost in comparison with fibre-blended MMCs [8]. Aluminium-based MMCs can be produced by liquid metallurgical stir casting methodology. Thus, many researchers focus on the influence of nanoparticles on the structure evolution in matrix alloy [9]. The procedure for fabricating the MMCs had a strong dominance on the tribological and mechanical characteristics of any material [10]. The mechanism of conventional casting came into actuality in 1968 by Ray [11], when he stirred the molten alloy of aluminium by encompassing alumina ceramic particulates into the melt, and in this process, the discontinuous reinforcement phases are incorporated into a matrix formed by a mechanical stirrer. Jiang et al. [12] investigated the creep and morphological aspects of high-pressure die-cast Mg–9Al–1Zn–1Sr alloy at 130 to 170°C and stresses from 30 to 80 MPa. The rate of creep at 70 MPa enhanced, and thus, a tertiary stage was noticed. The majority of the intermetallic regions were proliferated on the eutectic zones so that they constituted a continuous reticular region. The origin of the threshold stress could be confederate with the Orowan strengthening of γ-$Mg_{17}Al_{12}$ platelets that dynamically precipitated in the magnesium. Dai et al. [13] synthesized in situ TiB_2/$Al_{12}Si_4Cu_2NiMg$ (mentioned as "Al-12Si") composite processed by salt metal reaction methodology. The influence of reinforcements in wt% and heat treatment on creep deformation was evaluated at 632 K under steady force in the air. It was also noticed that the steady-state rate of creep was minimal at 4 wt% TiB_2/Al-12Si composite. The creep dislocation of the 4 wt% TiB_2/Al-12Si composite material was influenced by the climb of dislocations in the matrix. Coyal et al. [14] investigated various mechanical wear aspects of AA6061 alloy blended with jute ash (50 μm) and SiC (10 μm) reinforcements using conventional casting techniques. The tensile behaviour of the developed hybrid MMCs drastically enhanced because of the strongly bonded ceramic material in the matrix. Enhancement in microhardness can be attributed to the dynamic process of recovery and recrystallization. Wear resistance was mainly dependent on the hardness of the material. Onoro et al. [15] estimated the high-temperature mechanical properties such as hardness and tensile of AA6061 and AA7075 reinforced with boron carbide particles. All the composites were prepared by hot extrusion. Microstructural analysis reveals that the chemical reactions that occur may alter the interfacial characteristics of AMCs. Diffusion mechanism was found to be influential betwixt reinforcements and matrix. At 200 to 300°C, the tensile performance reduces drastically due to the matrix that loses the aging heat treatment by growing coherent hardened precipitates with a subsequent softening. From 200 to 400°C, the mechanical aspects of the 7015 alloy diminish more drastically than those of the 6061 alloy. The interaction betwixt the particulates and dislocations leads to an increment in strength, which is consorted with the Orowan mechanism. Sethi et al. [16] synthesized and characterized AA7075 reinforced with TiB_2 formed through stir casting. It was noticed that TiB_2 particles were homogeneously disseminated in both intra- and intergranular regions and an insignificant quantity of agglomeration was seen at 9 and 12 wt%, respectively. Reduction in grain size results in an increase in microhardness with an increment in wt% of the reinforcements. Strength due to the tension was found to be enhanced due to the restriction of cracks by reinforcements due to its load bearing capacity.

The mechanical characteristics at ambient and elevated temperatures of AA7075-based multihybrid MMCs blended with hard ceramic particulates have been extensively examined. Therefore, in the present research paper, AA7075 matrix composites were fabricated through a low-cost conventional stir casting technique by adding Si_3N_4, TaC, and Ti particles as reinforcement particles. Eventually, there are several facts on the influence of wt%, shape, size, and orientation of the reinforcements on the failure modes and fracture approach. Moreover, literature represent minimal information on the effects of Si_3N_4, TaC, and Ti particulates as blended MMCs at escalated temperatures. In our present research work, tantalum carbide (TaC) is one of the primary and most expensive ceramic reinforcement materials that could serve the purpose of withstanding high temperatures. Therefore, for low economy applications, this particular reinforcement cannot be used. In order to enhance the hardness above a particular limit, the material becomes more brittle. Therefore, the material may not be suitable for applications such as heavy cutting tools due to its extreme hardness. AA7075 reinforced hybrid MMCs can be utilized for all other engineering applications related to high- and low-temperature environmental conditions. Therefore, this research article aims to attain the optimum combination of the reinforcements in the AA7075 matrix material and estimate the influence of temperature on the mechanical behaviour of AA7075 multihybrid MMCs blended with distinct wt% of Si_3N_4/TaC and Ti particulates. Furthermore, a detailed experimental study on microstructural, high temperature tensile, creep, and low-cycle fatigue characterization of fabricated MMCs (AA7075) was carried out for the proposed hybrid MMCs.

2. Materials and Its Processing Technology

2.1. Material Preference. Aluminium-zinc alloy is also called aluminium 7000 series alloy because of the utmost zinc quantity proportion betwixt 5.1 and 6.1 percentages. In 1943, these series were first confidentially evolved by the Japanese company, Sumitomo Metal, ultimately for the manufacturing of the airframe in the Imperial Japanese Navy [17]. In the present study, AA7075 grade has been utilized as a base alloy for setting up aluminium-based hybrid MMCs using the conventional stir casting technique. This material was chosen as a matrix because of its high weight to strength proportion, high strength, less density, minimal cost, and exceptional material quality, which are generally encountered by the scientists for defence, military, armor, marine,

and automobile applications [18]. Table 1 displays the description of the chemical configuration of the AA7075 matrix utilized in the fabrication of the hybrid MMCs. The density of MMCs plays a crucial role in selecting the material for functional and structural applications, particularly for marine and automobile sectors.

Table 2 shows the various physical, mechanical, and thermal properties of the selected matrix and reinforcement materials. Ceramic reinforcement materials such as Si_3N_4, TaC, and Ti were chosen to improve various desired mechanical, fatigue, and creep characteristics of the proposed MMCs. The selected reinforcement particles were acquired from Saveer Matrix Nano Private Limited, Greater Noida, Uttar Pradesh, India. Table 3 shows the various proportions of matrix and reinforcements used for this research. Hard ceramic particles such as Si_3N_4 act as solid lubricants that enhance the tribological behaviour of materials and are a good replacement for graphite. Si_3N_4 was selected as reinforcement that provides sustainability at high temperatures [19]. Si_3N_4 particulates of 99.9% fineness with 20 μm particulate size were chosen. TaC is an appealing material among the transition metal carbide. The interest in TaC has been growing in recent years due to its wide applications in industry as cutting tools and hard coatings owing to its chemical inertness, high hardness, and exceptional corrosion resistance and more essentially its ability to form solid solutions [20]. TaC of 99.9% purity with 200–250 nm was used for this research. Ti is very hard compared with aluminium, and more essentially, it does not have to fend for any chemical reaction with aluminium to form any reactive product. Due to the enhanced specific strength and corrosion resistance in aggressive media, certain aluminium alloys can operate in corrosive environments without any strong restrictions on their service life. This particular set of characteristics makes aluminium alloys the material of selection for the needs of the automobile industry in several applications. The titanium of 99.9% purity with 70 µm particulate size was utilized for this present study. The range of reinforcements as shown in Table 3 was finalized based on previous literature.

2.2. Preparation of Materials. In the present experimental investigation, liquid metallurgical stir casting methodology was utilized for fabricating MMCs. The uniform dissemination of added ceramic particles in the matrix was acquired by the pertinent mechanical stirring route. In the inducement, the predefined wt% of AA7075 was partitioned from bar stock and heated to a molten state in the electric muffle furnace. Table 4 shows the detailed and optimum process parameters utilized [21] for developing the multihybrid MMCs. Furthermore, Si_3N_4, TaC, and Ti particles were preheated to about 250 and 300°C accordingly before inclusion in the smelted metal. Once the metal reached the semiliquid state, the preheated ceramic particulates of Si_3N_4, TaC, and Ti with distinct wt% were added to the matrix to fabricate AA7075/Si_3N_4/TaC/Ti MMCs, respectively.

It is pivotal to observe that the mechanical mixing was executed at a pace of 200 rpm every 2 to 3 minutes to validate the homogeneous dispersion of Si_3N_4, TaC, and Ti particulates in the AA7075 matrix. Once the blending of alloy in the liquid form was completed, it was sluiced into the preheated casting mould through a preheated run-away channel and allowed it to solidify. A similar approach was repeated with distinct wt% of Si_3N_4, TaC, and Ti, and multihybrid aluminium MMCs were prepared accordingly. Once the composite mould was cooled at ambient temperature, various testing specimens were adapted in accordance with ASTM standards.

3. Experimentation

3.1. Density and Porosity Examination. Density is a significant parameter that reflects the quality and desired characteristics of the composite materials. Experimental and theoretical densities were obtained to estimate the percentage porosity of the developed multihybrid MMCs. Theoretical and experimental densities were evaluated using the rule of mixtures and Archimedes' principle. By computing the mass and volume of the composite samples, the densities can be quantified. With such a simple approach, even the closed porosity will be considered into account. Sample sizes of $20 \times 10 \times 10\ mm^3$ were utilized for examining both experimentally and theoretically densities according to the ASTM D792 standard.

3.2. Microstructural Analysis. The square samples with $10 \times 10 \times 10\ mm^3$ were processed to inspect the microstructural of the manufactured hybrid MMCs according to ASTM standards as shown in Figure 1. To polish the test samples, distinct grades (400, 600, 1,000, and 1,200) of emery papers were utilized. In continuation with that distinct grade of diamond, paste was applied on the samples and polished utilizing a twin-disc polisher machine to obtain a shiny surface. Keller's reagent was etched on the specimens to disclose the grain boundaries and eliminate impurities. An optical metallurgical microscope (Model: QS Metrology, XJL–17) was utilized for examination as displayed in Figure 2(a). As shown in Figure 2(b), scanning electron microscope (SEM), X-ray diffraction (XRD), and energy-dispersive X-ray spectroscopy (EDX) were performed to confirm the homogeneous dissemination of reinforcements and to observe the occurrence of morphology and structure of reinforcement particulates in the AA7075 alloy.

3.3. High-Temperature Tensile Analysis. Tensile experiments were conducted to evaluate the tensile nature (percentage elongation, yield point, ultimate point, and breakpoint) of the selected AA7075 and fabricated hybrid MMCs. High-temperature tensile experiments have been conducted at ambient conditions (30°C, 60°C, 90°C, and 120°C). For elevated-temperature tensile analysis, an induction coil sort of heating furnace with an attached temperature control arrangement was developed and utilized for heating the tensile specimens. The temperature was measured directly on samples that were heated until their temperature stabilized at the required level. The specimens were held at the set point temperature for half an

Table 1: Chemical arrangement of AA7075.

Particulars	Si	Fe	Cu	Mn	Mg	Cr	Zn	Ti	Ni	Zr	Al
Minimum (wt%)	0.4	0.5	1.2	0.3	2.1	0.18	5.1	0.10	0.01	0.02	Balance
Maximum (wt%)			2.0		2.9	0.28	6.1				

Table 2: Properties of matrix and reinforcing phase.

S. No.	Properties	Matrix	Reinforcement materials		
		AA7075	Si_3N_4	TaC	Ti
1	Density (g/cm^3)	2.81	3.17	14.3	4.506
2	Melting point (°C)	700	1900	3900	1668
3	Hardness	60–150 BHN	13.5–20 HV	830–2340 HV	2,200 BHN
4	Elastic modulus (GPa)	70–80	28–46	537	106 psi
5	Tensile strength (MPa)	280	490	—	345

Table 3: Control factors – stir casting process.

S. No.	Quantity of matrix (wt%)	Quantity of reinforcements (wt%)		
	AA7075	Si_3N_4	TaC	Ti
C1	100	0	0	0
C2	95.75	2	0.25	2
C3	94	4	0.5	1.5
C4	92.25	6	0.75	1
C5	90.5	8	1	0.5

Table 4: Control factors – stir casting process.

S. No.	Processing conditions	Values
1	Time for stirring	5 minutes
2	Stirring speed	200 rpm
3	Temperature of melt	650°C
4	Temperature during stirring	670 to 700°C
4	Preheating temperature	250 to 300°C
5	Crucible size/company	4/bell
6	Maximum temperature of the furnace	750°C
7	Type of furnace	Electric muffle furnace
8	Mould size	$100 \times 100 \times 10$ mm^3

hour for homogeneity before loading the actual experiments. The operating temperature of the test samples was perceived by thermocouples during experimentation. The UTS of the matrix and developed MMCs were premeditated using a digitalized universal testing machine (UTM) as displayed in Figure 3 with 50 kN of ultimate load. In accordance with the ASTM E8 standard, the specimens as shown in Figure 4 were shaped and clamped in the UTM machine and pulled until deformation. During the analysis, the load applied and the displacement together with the sample deformation was recorded using a high-temperature extensometer. Later, the load and displacement plots were brought about on a computer that was synchronized with the machine. Using load and area of the tensile test samples, UTS was obtained at a distinct temperature range. Experiments were performed five times to ensure repeatability and average was considered.

3.4. Low-Cycle Fatigue Strength Analysis. Fatigue is an important characteristic of the material put through cyclic loading failure used to achieve robust performance. Considerable plastic distortion and short lifetime corresponds to low-cycle fatigue. Primarily in the loading region, the materials suffer distortion in an undistinguishable manner. The fatigue test samples as shown in Figure 5 were developed as per ASTM E606 with a gauge length of 40 mm. The fatigue test was conducted on a computerized fatigue testing machine (AVG Engineering Pvt. Ltd., Coimbatore, Tamilnadu, India) as shown in Figure 6 with tension-compression cyclic loading of 30 to 40 cycles/min and an uttermost force of 1 ton. The prepared fatigue test samples were equipped axially and clamped rigidly to the fixtures. The load was applied to the specimens, and then the cycle to failure was established. The experiments were carried out at an ambient temperature and prolonged till the final fracture. Fatigue life (N_f) was considered as the number of cycles to cause complete failure. Based on the load applied and stress obtained, S-N curves were plotted for different weight fractions of hybrid MMCs. An average of five outcomes was examined as fatigue life (N_f) of each sample.

3.5. Elevated Temperature Creep Analysis. Creep is stated as the accelerating fracture of material under the action of a steady force. Creep occurs as the result of prolonged exposures to stresses that are below the yield strength of the material. Since the mechanisms implicated in creep are thermally stimulated, creep does not become considerable until temperatures of the order of 0.3 T_m for pure metals and 0.4 T_m for alloys. Creep test samples were shaped as per ASTM E139 as shown in Figure 7. Tensile creep analysis was executed at 423.15 K under constant applied stress in the limit of 40 to 60 MPa on the time-dependent creep testing equipment (AVG Engineering Pvt. Ltd., Coimbatore, Tamilnadu, India) as displayed in Figure 8. Before clamping the specimens into the creep test machine, all the specimens were precisely polished to diminish the influence of machining deficiency. The temperature of the specimens was quantified utilizing a separate thermocouple that was attached exactly at the middle of the gauge length inside the

Figure 1: Test specimens for microstructural analysis.

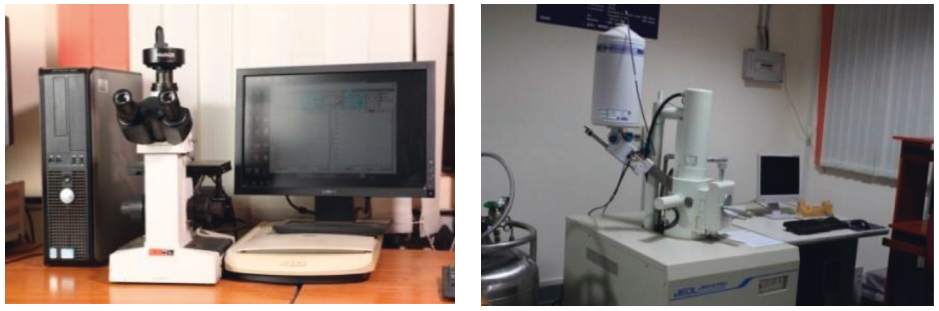

(a) (b)

Figure 2: Microstructural test setup: (a) optical microscope and (b) scanning electron microscope.

Figure 3: Universal tensile testing machine attached with heating chamber and temperature controller (Model: CUTM-50 kN).

heating furnace as shown in Figure 8. The strain was measured using an extensometer, and the data acquisition was formulated every 60 seconds during the entire experiment. All specimens were kept steady at the target temperature; the constant temperature was maintained for 10 minutes; and then the steady load was applied until failure. The rupture time was recorded, and the strain was calculated. Creep plots (strain vs. creep time) for the developed multihybrid MMCs at the different compositions of reinforcements was obtained experimentally.

4. Results and Discussion

4.1. Metallographic Aspects of AA7075/TaC/Ti/Si_3N_4 Hybrid Composites. The SEM analysis was done to obtain good-quality microstructural images on the surface of the base alloy and the fabricated MMC specimens. Figure 9 shows the SEM micrographs of various compositions of cast AA7075 reinforced with TaC/Ti/Si_3N_4 hybrid metal matrix composites. There is good dissemination of TaC, Ti, and Si_3N_4 ceramic particles over the AA7075 interface. This authenticates to the effectiveness of the liquid metallurgical stir casting route used in manufacturing the MMCs. Figure 9(a) displays the micrographs of the cast AA7075 matrix; it was evident that the entire grey region represents the matrix without reinforcement. As the particulate of TaC/Ti/Si_3N_4 is amalgamated into the melt pool of the molten metal (AA7075), a whitish region was noticed that depicts the occurrence of foreign ceramic particulates (TaC/Ti/Si_3N_4) embedded in the matrix alloy shown in Figures 9(b) to 9(e). It is justifiable to note that as the wt% of the particulate enhances, the whitish region becomes heavy and well disseminated homogeneously. From the SEM micrographs, it was observed that there were no voids, and cracks were identified on the matrix, which ensured the unblemished bonding betwixt reinforcement and matrix. The strong intermetallic bonding, exceptional wettability betwixt the discontinuous reinforcement phase and continuous metal phase, and the homogeneous dissemination [22, 23] can be endorsed as the optimum process parameters utilized through the liquid metallurgical route.

Figure 10 shows the EDAX pattern of the AA7075 alloy and the developed multihybrid composite material. The EDAX pattern clearly reveals various elements present in the composite material. Figure 10(a) clearly reveals the presence of Mg, Al, and

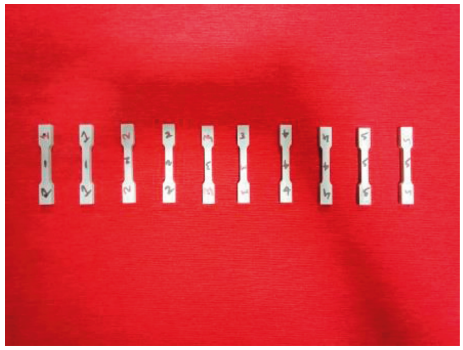

Figure 4: Test samples for tensile strength analysis.

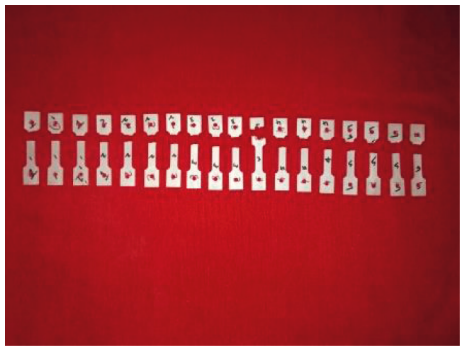

Figure 5: Fatigue test samples as per ASTM.

Figure 6: Hydraulic universal fatigue and creep testing machine (Model: AVJ-10T).

Zn as the primary alloying elements that provide additional strength and enhanced characteristics of the material. Additionally, EDAX pattern of the developed multihybrid MMCs is displayed in Figure 10(b), and various reinforcing elements such as Ta, C, Zn, C, and Cu can be clearly seen. This EDAX compositional analysis has been used to confirm the elemental presence. Since magnesium and silicon are major alloying elements, secondary precipitates such as Mg_2Si can be observed from the SEM analysis of the developed hybrid MMCs.

4.2. Density and Porosity Analysis of AA7075/TaC/Ti/Si_3N_4 Hybrid Composites. The density of MMCs primarily reckons on various attributes for instance nature, orientation, shape, and size of the reinforcement particulates. In the current exploration, the porosity of the manufactured MMCs has been inspected both theoretically and experimentally. Figure 11 shows the combined variation in theoretical, experimental densities, and percentage porosity of the developed AA7075/TaC/Ti/Si_3N_4 multihybrid composite materials. The obtained results reveal that the selected reinforcement materials such as TaC, Si_3N_4, and Ti have an infinitesimal influence on the overall density of the developed multihybrid composite materials. Due to the hard nature of the selected ceramic reinforcements, the overall density of the developed composite materials was found to be higher [24]. Since the density of the Si_3N_4 is comparatively higher with 3.44 g/cm^3 when compared to other reinforcements, it has a greater influence on the density of the hybrid composites. The AA7075 base alloy showed the experimental and theoretical density of 2.80 g/cm^3 and 2.81 g/cm^3, respectively, and porosity of 0.3559%. When ceramic reinforcement particulates were mixed with AA7075 base alloy (2.80 g/cm^3), the developed composite showed higher density with a reasonable amount of porosity. From the obtained experimental outcomes, it was observed that AA7075 reinforced with 8 wt% Si_3N_4, 1 wt% TaC, and 0.5 wt % Ti (sample C5) enhanced the experimental and theoretical densities up to 3.2464 g/cm^3 and 3.3038 g/cm^3 with maximum porosity of 1.7758%. This clearly shows that the increment in the density of the MMCs may be ascribed to the high density of Si_3N_4 than that of AA7075. This rise in porosity may be due to the existence of impurities in both the matrix material and reinforcement particulates. It can be inferred that because of the increment in wt% of distinct percentage compositions of hybrid MMCs, there has been an enhancement in cohesive bonding betwixt the matrix and the reinforcements. Also, because of the discrepancy in wt% of the hard particulates by performing steady stirring, the dispersoid concentration has been homogeneous with a minimal amount of porosity, and no enormous clustering has been noticed. It has been stated that [25] due to the increment in weight percentage of the reinforcements, the dissemination is more dependable with insignificant porosity.

4.3. High-Temperature Tensile Behaviour of AA7075/TaC/Ti/Si_3N_4 Hybrid Composites. Figure 12 displays the deviation of UTS of the developed composite materials concerning various operating temperatures (30, 60, 90, and 120°C). The outcomes are the average data depending on the indistinguishable tests. AA7075 matrix aluminium alloy is stronger, with and without TaC, Ti, and Si_3N_4 reinforced particles, at every temperature. It can be concluded that at higher temperatures, the UTS of the fabricated multihybrid MMCs was more than that of the base metal, which means that the ceramic reinforcements can withstand the temperature by developing a strong bond between the matrix and reinforcements. At ambient temperature (30°C), the MMCs

Figure 7: Creep test samples as per ASTM standard.

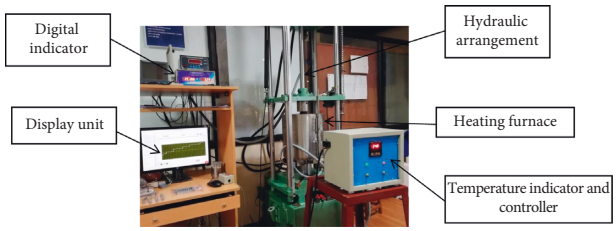

Figure 8: Time-dependent creep experimental test equipment.

showed an improved tensile strength of 137.64 N/mm^2. Later, when the temperature enhances from 30°C to 60°C, the composite material with 0.5 wt% TaC, 4 wt% Si_3N_4, and 1.5 wt% Ti showed a higher tensile strength of 230.07 N/mm^2. When the temperature reached beyond 100°C, the composite material with 0.75 wt% TaC, 6 wt% Si_3N_4, and 1 wt% Ti proved to have a higher strength of 232.17 N/mm^2. This shows that ceramic reinforcement has the capability of operating at higher temperatures. The tension properties enhance as anticipated, but the process is not homogeneous, owing to the fact that several metallurgical phenomena are embroiled synchronically [26]. At room temperature (30°C), it was noticed that the tensile strength of the fabricated MMCs enhanced; it implies that ductility has upgraded with the introduction of reinforcements. This revamp in ductility can be justified by proper dissemination and abutting packing of the reinforcement particulates in the AA7075 alloy. Also, improved tensile strength was observed at elevated temperatures. The selected ceramic reinforcement particulates increase the mechanical characteristics of matrix alloy over the consolidated temperature. The TaC, Ti, and Si_3N_4 particles improve the tensile properties at distinct temperatures primarily by stress transference from the aluminium ally to the reinforced ceramics [27]. The interactivity betwixt the dislocations and particulates culminates in enhancement in strength, which is syndicated with the Orowan strengthening procedure [28] by which a dislocation bypasses impervious obstacles, where a dislocation bows out tremendously to leave a dislocation loop around a particulate.

4.4. Morphology of the Fractured Tensile Samples. Figures 13(a) and 13(b) depict the SEM analysis of the fractured AA7075 tensile samples reinforced with 1wt%TaC/8wt%Si_3N_4/0.5wt%Ti at 30 and 120°C. Dispersed and pulled out TaC/Si_3N_4/Ti ceramic particulates was observed on the fracture sample of the developed composite material. At ambient conditions, the composites exhibit uniform or notched features, indicating the preferential ductile mechanism of MMCs. At escalated temperatures, bonding of ceramic particulates can be observed from the fractured tensile samples. As percentage elongation depicts the ductile nature of the material, the composite with 1wt%TaC/8wt%Si_3N_4/0.5wt%Ti reinforcement was more ductile in nature without the decline in tensile behaviour of the developed composite material.

4.5. Low-Cycle Fatigue Behaviour of AA7075/TaC/Ti/Si_3N_4 Hybrid Composites. Figure 14 displays the typical deviation of low cycle fatigue stress versus a number of cycles. From the obtained experimental outcomes, enhanced fatigue life was observed from the developed hybrid MMCs by operating at higher number of cycles. Especially, the addition of Si_3N_4 improved the fatigue life of the composites. This can be attributed to the occurrence of hard ceramic particulates with homogeneous distribution throughout the alloy material. The MMCs with AA7075 reinforced with 0.5 wt% TaC, 4 wt% Si_3N_4, and 1.5 wt% Ti proved to operate at a higher number of cycles of 14×10^3 cycles with maximum elongation of 0.180 mm. This inspection is in good agreement with the outcomes of Senthil Kumar et al. [29] who disclosed the low-cycle fatigue characteristics of AA2014-Al_2O_3 hybrid MMCs. The above manifestation can be validated to the dislocation slip-dominated distortions on account of tension-compression distortion due to the AA7075 matrix material whose structure is face-centred cubic. This is an outcome of cyclic hardening of successive cycle distortions. AA7075/TaC/Ti/Si_3N_4 MMCs display a balanced plastic strain for the cyclic contortion. Reduction in porosity and higher yield strength of the MMCs attributed to enhanced fatigue life. In addition to this, the excellent bonding betwixt matrix and reinforcement and finer grain size [30] is also a crucial parameter, which inveigled the improved resistance to fatigue of the manufactured MMCs.

4.6. Morphology of the Fractured Fatigue Samples. Figure 15 displays the fractured fatigue sample of AA7075 and the developed multihybrid MMCs. All the fracture

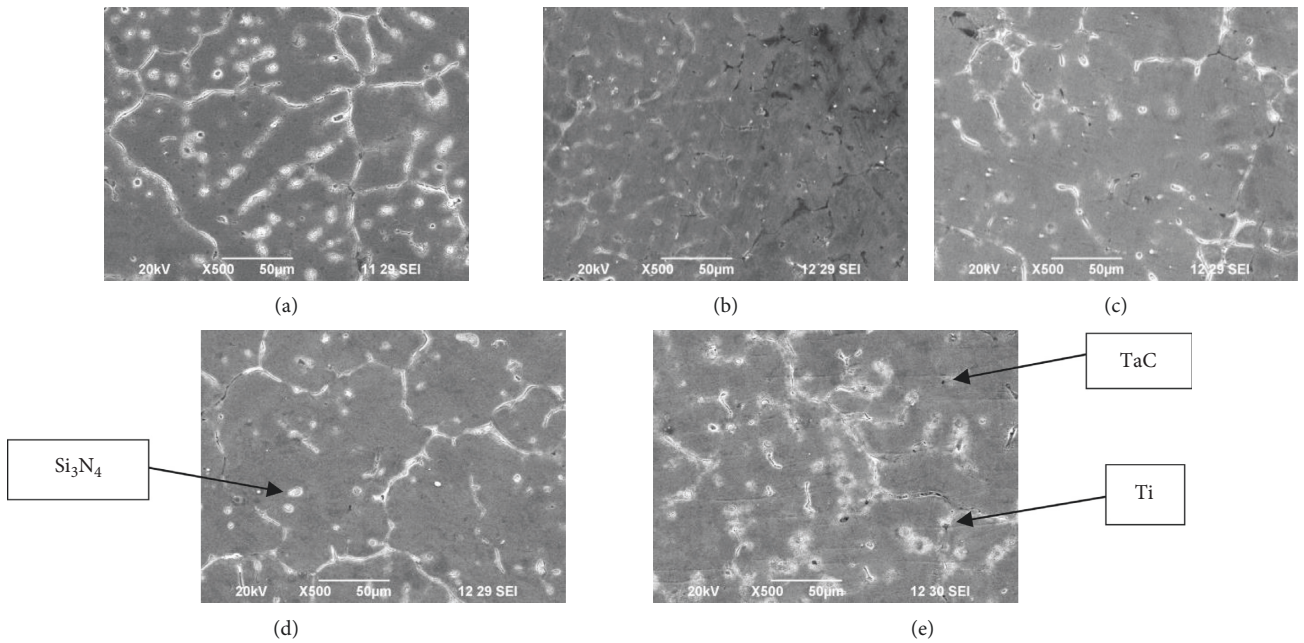

Figure 9: SEM morphology of the developed composites: (a) pure AA7075, (b) AA7075 + 0.25wt%TaC + 2wt%Si_3N_4 + 2wt%Ti, (c) AA7075 + 0.5wt%TaC + 4wt %Si3N4 + 1.5wt%Ti, (d) AA7075 + 0.75wt%TaC + 6wt% Si_3N_4 + 1wt%Ti, and (e) AA7075 + 1wt%TaC + 8wt% Si_3N_4 + 0.5wt%Ti.

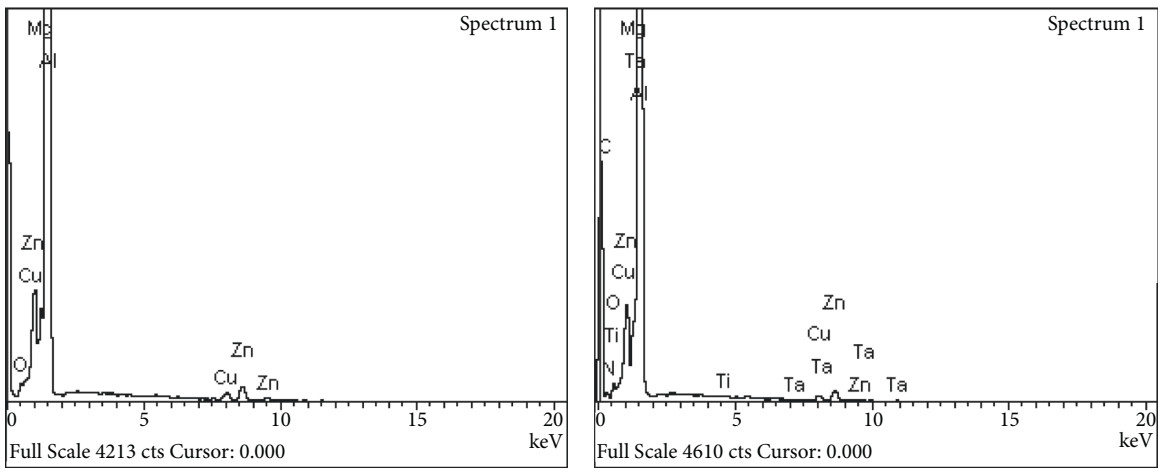

Figure 10: EDAX pattern of (a) AA7075 and (b) AA7075 + 1wt%TaC + 8wt%Si_3N_4 + 0.5wt%Ti.

composite samples are composed mostly of dimples with the TaC/Si_3N_4 and Ti particle clusters inside. At lower exacerbation, the fractured creep sample of AA7075 alloy was observed as displayed in Figure 15(a). Various morphological parameters such as crack instigation, near crack instigation site, and fast fracture surface were evidently noticed and evaluated. The occurrence of severe clusters has caused irregular dimples with distinct sizes, demonstrating the detrimental influence on the creep resilience. It is obvious that the larger size of such a brittle phase is detrimental to creep life. At last, the enhanced dislocation density at the edges and corners of reinforcements may quicken the breakdown of the brittle phase, which should reduce the creep resistance of the AA7075/Si_3N_4/TaC/Ti hybrid composite in this work. Also, it displays the occurrence of fracture surfaces with limited dimple structure and more reinforcement particles. It indicates the presence of a stronger reinforcement and matrix interface. Figure 15(b) shows the crack growth near the initiation site occurred primarily in the matrix phase material. There is an excellent particle and matrix interface cracking or reinforcements cracking, and a fast fracture site was also evidently noticed. It is also presumed that the dimple density of the MMCs was more than that of the AA7075 alloy.

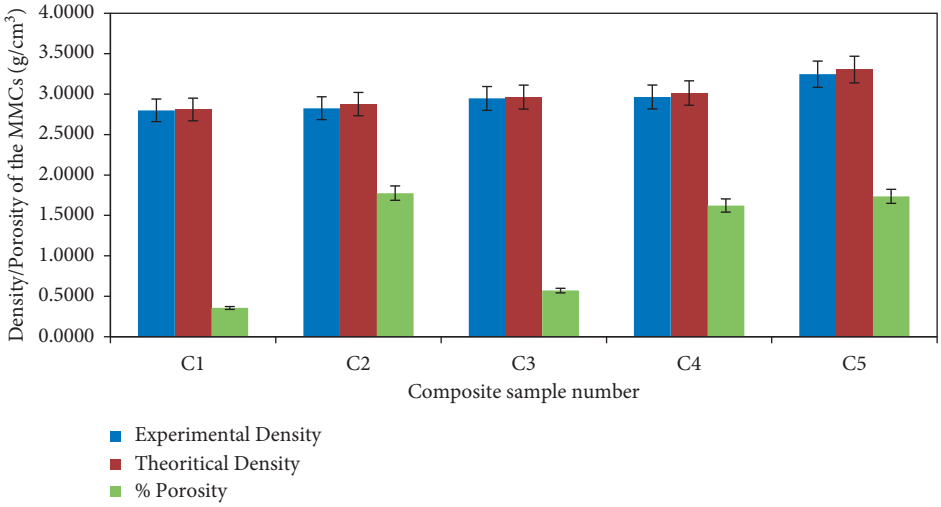

Figure 11: Deviation of density and percentage porosity of the developed hybrid MMCs.

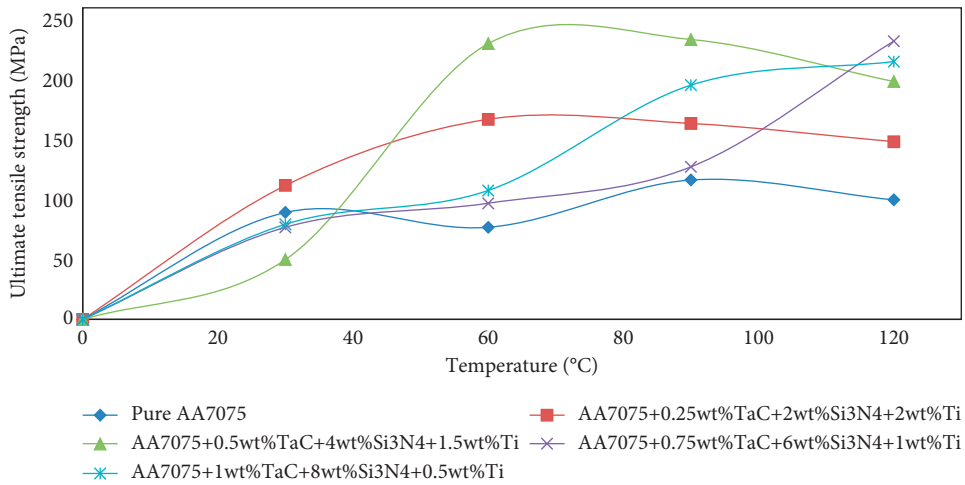

Figure 12: Deviation of UTS versus temperatures of the developed MMCs.

4.7. Creep Deformation of AA7075/TaC/Ti/Si_3N_4 Hybrid Composites. Figure 16 shows the change in displacement with respect to time of rupture for various compositions of aluminium-based MMCs. AA7075 alloy reinforced with 1 wt % TaC, 8 wt% Si_3N_4, and 0.5 wt% Ti operated at the higher period of time of 33,558 seconds with a maximum displacement of 2.61 mm. The higher weight fraction of Si_3N_4 and TaC showed higher creep strength with a minimum amount weight fraction of titanium. The creep strength of the developed MMCs enhanced due to the homogeneous dissemination of Si_3N_4/TaC/Ti particulates over the matrix alloy. This shows that the secondary creep stage is more lineated with the addition of Si_3N_4/TaC/Ti. Sample C3 with AA7075 reinforced with 0.5 wt% TaC, 4 wt% Si_3N_4, and 1.5 wt% Ti operated at a minimum time period but elongated up to 16.08 mm showed the ductile nature of the material. This can be attributed to the advent of damage mechanisms [31] within the matrix such as the prevalence of debonding at the interfaces between the reinforcement and matrix.

4.8. Morphology of the Fractured Creep Composite Samples. Figures 17(a) and 17(b) display the SEM microstructure of the deformed creep samples of AA7075 and the developed hybrid composites at constant stress and temperature. Exceptionally, for those on the prior austenite grain boundaries and on the lath boundaries, the morphology of the fractured samples discloses eminent coarsening of the precipitates. The fractured morphology reveals cup and cone fractures as shown in the microstructure. The justification for this catastrophe is that the creep deformation (or cracks) develops inwards after instigating the outer layer of the sample. The presence of many voids was noticed in the central equiaxed regions. Figures 17(a) and 17(b) show few areas of small pores filled with ceramic reinforcement particulates. The AA7075/TaC/Si_3N_4/Ti cyclic creep samples disclose regular transgranular fracture ensuing from microvoid coalescence. It was noticed that in the time-dependent creep analysis, all of the ruptured specimens exhibit similar transgranular fractures [32] regardless of the creep experimental

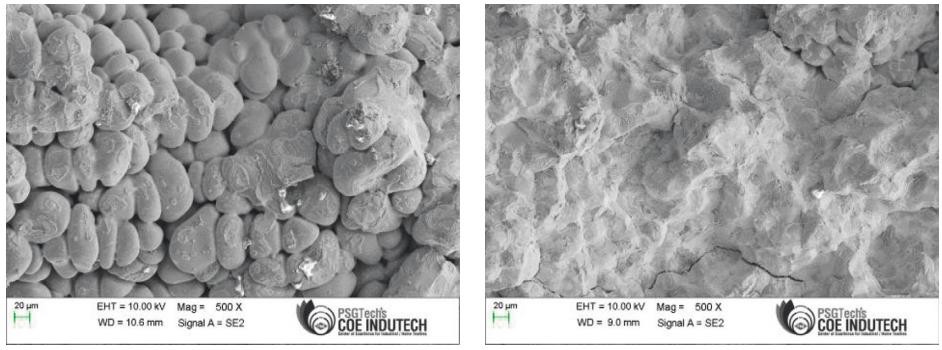

(a) (b)

Figure 13: SEM morphology of fractured AA7075/1wt%TaC/8wt%Si_3N_4/0.5wt%Ti tensile sample: (a) 30°C and (b) 120°C.

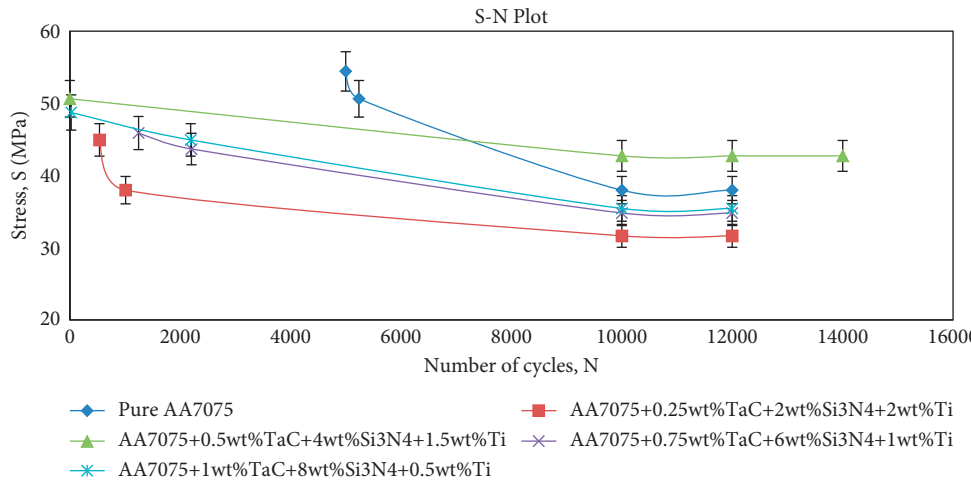

Figure 14: Deviation of cyclic stress with respect to the number of cycles.

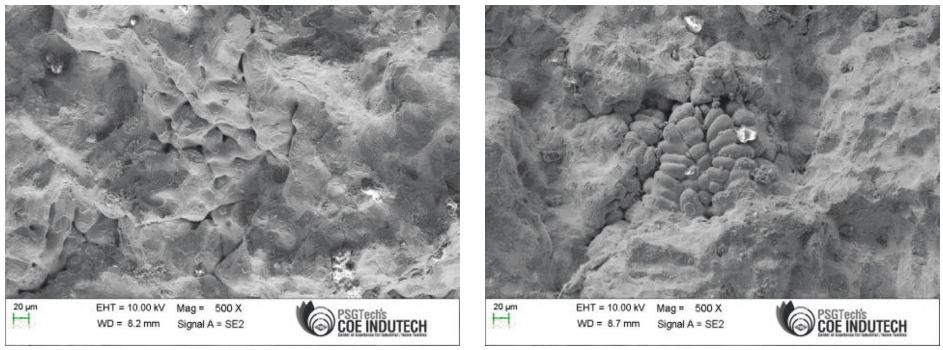

(a) (b)

Figure 15: SEM analysis of fractured fatigue samples: (a) AA7075 and (b) AA7075/0.5wt%TaC/4wt% Si_3N_4/1.5wt% Ti.

conditions. An increase in the coarsening kinetics was notable with an increment in temperature, for extended creep exposures. However, in the case of elevated temperature creep analysis with shorter rupture lives, the lath structure within the prior austenitic grain boundaries did not display much change on a macroscale.

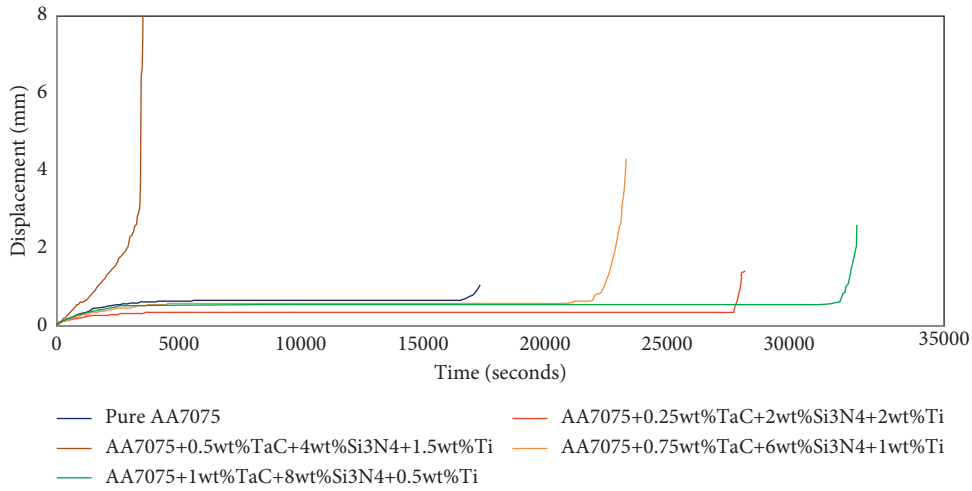

Figure 16: Variation of strain with respect to time of rupture of MMCs.

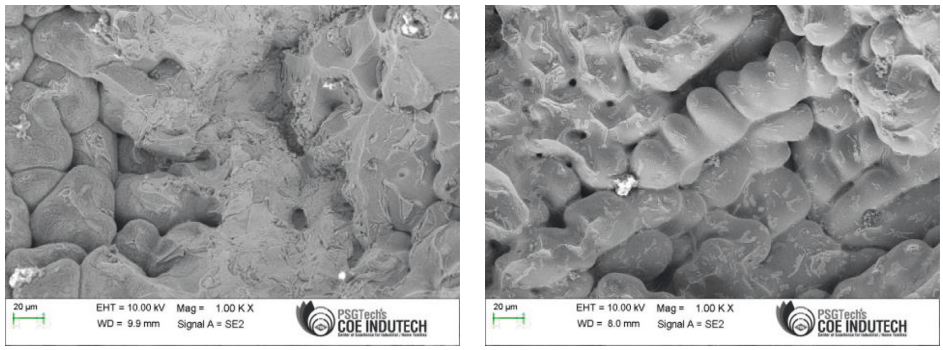

(a) (b)

Figure 17: SEM analysis of fractured creep samples: (a) AA7075 and (b) AA7075/1wt%TaC/8wt% Si_3N_4/0.5wt%Ti.

5. Conclusions

The traditional stir casting procedure was adopted in sprouting AA7075 reinforced with TaC/Ti/Si_3N_4 hard ceramic particulates. High-temperature tensile, fatigue, and creep deformation were inspected experimentally. The subsequent conclusions can be exploited.

(i) Microstructural study shows fairly homogeneous dissemination of TaC/Ti/Si_3N_4 in the AA7075 matrix material. The SEM interpretations also exhibited a ductile and brittle mode of terminations for pure AA7075 alloy and fabricated MMCs, correlatively.

(ii) SEM morphology also reveals good wettability and proper mixing. Strong interfacial bonding between the matrix and reinforcement material was observed, and this proves the optimum process parameters and the quality of the casting process.

(iii) Experimental and theoretical densities of the developed AA7075 reinforced with 8 wt% Si_3N_4, 1 wt% TaC, and 0.5 wt% Ti (sample C5) MMCs were found to be enhanced up to 3.2464 g/cm^3 and 3.3038 g/cm^3, respectively, with maximum porosity of 1.7758% because of the inclusion of hard particulates and excellent cohesive bonding among the reinforcement and matrix.

(iv) The tensile strength of the MMCs has been enhanced by the inclusion of hard ceramic particulates. Higher content of TaC/Si_3N_4/Ti improves the tensile nature of the MMCs at room temperature. Beyond 100°C, the MMCs with 0.75 wt% TaC, 6 wt% Si_3N_4, and 1 wt% Ti proved to have a higher strength of 232.17 N/mm^2. At elevated temperatures beyond 100°C, the material softening takes place beyond which the reinforcement enters the voids and pores thus restrict the crack propagation. At 30°C, uniform dimple features of

the composites indicates the preferentially ductile mechanism of the composite. At elevated temperatures, good bonding of ceramic particulates can be observed from the fractured tensile samples.

(v) Increased wt% of Si_3N_4/TaC/Ti improves the fatigue characteristics of the developed MMCs. AA7075 reinforced with 0.5 wt% TaC, 4 wt% Si_3N_4, and 1.5 wt% Ti proved to operate at a higher number of cycles of 14×10^3 cycles with maximum elongation of 0.180 mm. Due to the continuous cyclic deformation, cyclic hardening takes place. Reduction in porosity and higher yield strength of the MMCs attributed to improved fatigue life. The excellent bonding betwixt matrix and reinforcement and finer grain size is also a significant consideration, which influenced the improved fatigue resistance.

(vi) Creep analysis reveals that AA7075 blended with 1 wt% TaC, 8 wt% Si_3N_4, and 0.5 wt% Ti operated at the higher period of time of 33,558 seconds with a maximum displacement of 2.61 mm. This shows that the presence of reinforcement material proved sustainability at higher temperatures and at higher stress levels.

Data Availability

The data used to support the findings of this study are included within the article.

Conflicts of Interest

The authors declare that there are no conflicts of interest regarding the publication of this article.

Acknowledgments

This research work was not funded by any organization.

References

[1] M. Y. Zhou, L. B. Ren, L. L. Fan et al., "Progress in research on hybrid metal matrix composites," *Journal of Alloys and Compounds*, vol. 838, Article ID 155274, 2020.

[2] M. B. A. Shuvho, M. A. Chowdhury, M. Kchaou, B. K. Roy, A. Rahman, and M. A. Islam, "Surface characterization and mechanical behavior of aluminum based metal matrix composite reinforced with nano Al2O3, SiC, TiO2 particles," *Chemical Data Collections*, vol. 28, Article ID 100442, 2020.

[3] M. Gao, H. Kang, Z. Chen et al., "Enhanced strength-ductility synergy in a boron carbide reinforced aluminum matrix composite at 77 K," *Journal of Alloys and Compounds*, vol. 818, Article ID 153310, 2020.

[4] R. Manikandan, T. V. Arjunan, and O. P A. R. Nath, "Studies on micro structural characteristics, mechanical and tribological behaviours of boron carbide and cow dung ash reinforced aluminium (Al 7075) hybrid metal matrix composite," *Composites Part B: Engineering*, vol. 183, Article ID 107668, 2020.

[5] J. M. Mistry and P. P. Gohil, "Experimental investigations on wear and friction behaviour of Si3N4p reinforced heat-treated aluminium matrix composites produced using electromagnetic stir casting process," *Composites Part B: Engineering*, vol. 161, pp. 190–204, 2019.

[6] C. Kar and B. Surekha, "Characterisation of aluminium metal matrix composites reinforced with titanium carbide and red mud," *Materials Research Innovations*, vol. 25, no. 2, pp. 67–75, 2021.

[7] S. H. Park, D. H. Cho, K. M. Cho, and I. M. Park, "Creep properties of squeeze-infiltrated carbon nanotube and aluminum borate whisker reinforced AS52 Mg metal matrix composites," *Metals and Materials International*, vol. 24, no. 5, pp. 1162–1171, 2018.

[8] H. A. Al-Salihi, A. A. Mahmood, and H. J. Alalkawi, "Mechanical and wear behavior of AA7075 aluminum matrix composites reinforced by Al2O3nanoparticles," *Nanocomposites*, vol. 5, no. 3, pp. 67–73, 2019.

[9] S. Suresh, G. H. Gowd, and M. L. S. Deva Kumar, "Tribological behavior of Al 7075/SiC metal matrix nano-composite by stir casting method," *Journal - The Institution of Engineers: Series D*, vol. 100, no. 1, pp. 97–103, 2019.

[10] P. Loganathan, A. Gnanavelbabu, and K. Rajkumar, "Influence of ZrB2/hBN particles on the wear behaviour of AA7075 composites fabricated through stir followed by squeeze cast technique," *Proceedings of the Institution of Mechanical Engineers-Part J: Journal of Engineering Tribology*, vol. 235, no. 1, pp. 149–160, 2021.

[11] N. Panwar and A. Chauhan, "Fabrication methods of particulate reinforced Aluminium metal matrix composite-A review," *Materials Today Proceedings*, vol. 5, no. 2, pp. 5933–5939, 2018.

[12] B. Jiang, D. Zhang, C. Sun, N. Li, Y. Liu, and Z. Cao, "Microstructure evolution and creep behavior of high-pressure die-cast Mg-9Al-1Zn-1Sr alloy," *Materials Science and Engineering A*, vol. 766, Article ID 138388, 2019.

[13] S. Dai, Z. Bian, M. Wang et al., "The high-temperature creep behavior of in-situ TiB2 particulate reinforced Al12Si4Cu2-NiMg composite," *Metals*, vol. 8, no. 11, pp. 917–1016, 2018.

[14] A. Coyal, N. Yuvaraj, R. Butola, and L. Tyagi, "An experimental analysis of tensile, hardness and wear properties of aluminium metal matrix composite through stir casting process," *SN Applied Sciences*, vol. 2, no. 5, pp. 892–910, 2020.

[15] J. Oñoro, M. D. Salvador, and L. E. G. Cambronero, "High-temperature mechanical properties of aluminium alloys reinforced with boron carbide particles," *Materials Science and Engineering A*, vol. 499, no. 1-2, pp. 421–426, 2009.

[16] D. Sethi, S. Kumar, S. Choudhury, S. Shekhar, and B. Saha Roy, "Synthesis and characterization of AA7075/TiB2 aluminum matrix composite formed through stir casting method," *Materials Today Proceedings*, vol. 26, pp. 1908–1913, 2020.

[17] M. Imran and A. R. A. Khan, "Characterization of Al-7075 metal matrix composites: a review," *Journal of Materials Research and Technology*, vol. 8, no. 3, pp. 3347–3356, 2019.

[18] N. Ramadoss, K. Pazhanivel, and G. Anbuchezhiyan, "Synthesis of B4C and BN reinforced Al7075 hybrid composites using stir casting method," *Journal of Materials Research and Technology*, vol. 9, no. 3, pp. 6297–6304, 2020.

[19] J. Fayomi, A. P. I. Popoola, O. P. Oladijo, O. M. Popoola, and O. S. I. Fayomi, "Experimental study of ZrB2-Si3N4 on the microstructure, mechanical and electrical properties of high grade AA8011 metal matrix composites," *Journal of Alloys and Compounds*, vol. 790, pp. 610–615, 2019.

[20] C. Zhang, A. Loganathan, B. Boesl, and A. Agarwal, "Thermal analysis of tantalum carbide-hafnium carbide solid solutions from room temperature to 1400 °C," *Coatings*, vol. 7, 2017.

[21] B. Das, S. Roy, R. N. Rai, S. C. Saha, and P. Majumder, "Effect of in-situ processing parameters on microstructure and mechanical properties of TiC particulate reinforced Al-4.5Cu alloy MMC fabricated by stir-casting technique - optimization using grey based differential evolution algorithm," *Measurement*, vol. 93, pp. 397–408, 2016.

[22] P. S. Reddy, R. Kesavan, and B. Vijaya Ramnath, "Investigation of mechanical properties of aluminium 6061-silicon carbide, boron carbide metal matrix composite," *Silicon*, vol. 10, no. 2, pp. 495–502, 2018.

[23] C. Sivakandhan, G. Babu Loganathan, G. Murali et al., "Material characterization and unconventional machining on synthesized Niobium metal matrix," *Materials Research Express*, vol. 7, no. 1, Article ID 15018, 2020.

[24] T. Satish Kumar, G. Suganya Priyadharshini, S. Shalini, K. Krishna Kumar, and R. Subramanian, "Characterization of NbC-reinforced AA7075 alloy composites produced using friction stir processing," *Transactions of the Indian Institute of Metals*, vol. 72, no. 6, pp. 1593–1596, 2019.

[25] S. A. M. Krishna, T. N. Shridhar, and L. Krishnamurthy, "Computational investigation on thermal conductivity behavior of Al 6061-SiC-Gr hybrid metal matrix composites," *International Journal of Computational Materials Science and Engineering*, vol. 4, no. 4, Article ID 1550021, 2015.

[26] C. Zheng and W. Yu, "Effect of low-temperature on mechanical behavior for an AISI 304 austenitic stainless steel," *Materials Science and Engineering A*, vol. 710, pp. 359–365, 2018.

[27] F. Rezaei, M. G. Kakroudi, V. Shahedifar, N. P. Vafa, and M. Golrokhsari, "Densification, microstructure and mechanical properties of hot pressed tantalum carbide," *Ceramics International*, vol. 43, no. 4, pp. 3489–3494, 2017.

[28] K. Munir, C. Wen, and Y. Li, "Graphene nanoplatelets-reinforced magnesium metal matrix nanocomposites with superior mechanical and corrosion performance for biomedical applications," *Journal of Magnesium and Alloys*, vol. 8, no. 1, pp. 269–290, 2020.

[29] R. Senthilkumar, N. Arunkumar, and M. Manzoor Hussian, "A comparative study on low cycle fatigue behaviour of nano and micro Al 2 O 3 reinforced AA2014 particulate hybrid composites," *Results in Physics*, vol. 5, pp. 273–280, 2015.

[30] N. K. Bhoi, H. Singh, and S. Pratap, "Developments in the aluminum metal matrix composites reinforced by micro/nano particles - a review," *Journal of Composite Materials*, vol. 54, no. 6, pp. 813–833, 2020.

[31] Z. Wang and H. Xiao, "A simulation of low and high cycle fatigue failure effects for metal matrix composites based on innovative J2-flow elastoplasticity model," *Materials*, vol. 10, no. 10, p. 1126, 2017.

[32] V. Sklenicka, K. Kuchařová, M. Kvapilová, and M. Svoboda, "Factors influencing creep resistance in discontinuously reinforced magnesium metal matrix composites," *Metallic Materials*, vol. 53, no. 4, pp. 221–229, 2016.